Experimental Thermal and Fluid Science 48 (2013) 213–221

Contents lists available at SciVerse ScienceDirect

Experimental Thermal and Fluid Science

journal homepage: www.elsevier.com/locate/etfs

Thermal–hydraulic physical models for a Printed Circuit Heat Exchanger covering He, He–CO_2 mixture, and water fluids using experimental data and CFD

In Hun Kim [a,b], Hee Cheon NO [a,*]

[a] Department of Nuclear and Quantum Engineering, Korea Advanced Institute of Science and Technology, 373-1 Guseong-dong, Yuseong-gu, Daejeon 305-701, Republic of Korea
[b] Nuclear Engineering Program, Department of Mechanical and Aerospace Engineering, The Ohio State University, Columbus, OH, USA

ARTICLE INFO

Article history:
Received 21 December 2012
Received in revised form 6 March 2013
Accepted 10 March 2013
Available online 20 March 2013

Keywords:
PCHE
Heat transfer
Pressure drop
Thermal–hydraulics
Mixture gas

ABSTRACT

A Printed Circuit Heat Exchanger (PCHE) is considered as a promising candidate for the use of an intermediate heat exchanger (IHX) in High Temperature Gas-cooled Reactors (HTGRs), since PCHEs offer high effectiveness and a compact size. It has been reported that the use of binary mixture gas can increase the thermal efficiency and reduce the turbo-machinery size in HTGRs. We performed experiments and numerical analysis on the PCHE using a mixture gas with Helium (He) and CO_2. We suggested the procedure to develop the correlations of Fanning factor and Nusselt number for PCHE channel geometry through introducing the concept of the local pitch-averaged correlations. A Computational Fluid Dynamics (CFDs) code, FLUENT, was validated against the current Mixture–Water test data and used to get the local pitch-averaged correlations to develop the local pitch-averaged correlations of Fanning factor and the Nusselt number. Using the local pitch-averaged correlations based on the He–He, the He–Water, and the Mixture–Water test data, we proposed the single Fanning factor correlation and the single Nusselt number correlation.

1. Introduction

As one of the Gen-IV nuclear reactors, a High Temperature Gas-cooled Reactor (HTGR) has various energy applications such as electricity generation, hydrogen production, and even desalination water production. This integrated system which can produce Water, Hydrogen, and Electricity using Nuclear reactors is named WHEN system [1]. For the multiple heat applications in HTGRs, heat exchangers should be necessary. However, it might not be possible to use shell and tube-type heat exchangers for the Intermediate Heat Exchanger (IHX) in HTGRs, because low heat transfer coefficient of gas working fluid causes the large size of the IHX. Therefore, currently, a Printed Circuit Heat Exchanger (PCHE)™, which is manufactured by Heatric, is considered as one of promising candidates. According to a Heatric website [2], if the PCHE type is selected, the size can be highly reduced to the 1/5 or 1/6 size of the shell and tube-type heat exchanger.

The previous researches related to the PCHEs have been performed. In order to adopt the PCHEs to either the IHX or the recuperator in HTGRs, Kim et al. [3] investigated the thermal–hydraulic performance of PCHE experimentally and numerically using a He–He test facility and Computational Fluid Dynamics (CFDs) code, FLUENT. The correlations of Fanning factor and Nusselt number for the specific design of PCHE were proposed in laminar region. Kim and NO [4] developed some physical models of Fanning factor and Nusselt number according to the geometry, considering various angle, pitch, and diameter. Using them, the optimal IHX design through cost analysis was finally proposed. Kim and NO [5] investigated thermal–hydraulic performance of a PCHE in a He–Water test loop for the application of the PCHE to the pre-cooler in the HTGR. It was found out that the vertical operation of the PCHE is more stable than its horizontal operation. For the working fluids of helium and water, the correlations of Fanning factor and Nusselt number were proposed.

In addition, several researches regarding the use of binary mixture gases were carried out for the Brayton cycle of the HTGR. The number of stages in turbo-machines such as compressor and turbine decreases to 1/3 of the stages in the pure helium Brayton cycle, when He–Xe mixture with 15 g/mole was used [6]. Jeong et al. [7] showed that the use of a mixture gas can increase the overall thermal efficiency of gas cooled reactors due to the changes of properties and critical points. Until now, thermal–hydraulic performance evaluations on the PCHE in the mixture gas condition were not investigated. Therefore, we need to investigate the mixture gas behavior in the PCHE, for example, whether the mixture gas follows the correlations developed previously in the single working fluid or not.

* Corresponding author. Tel.: +82 42 350 3817; fax: +82 42 350 3810.
E-mail addresses: kim.4704@osu.edu (I.H. Kim), hcno@kaist.ac.kr (H.C. NO).

0894-1777/$ - see front matter © 2013 Elsevier Inc. All rights reserved.
http://dx.doi.org/10.1016/j.expthermflusci.2013.03.003

Nomenclature

Q	heat load (W)
$\dot{m}$	mass flow rate (kg/s)
v	velocity (m/s)
T	temperature (K)
c_p	specific heat capacity (kJ/kg K)
c_{p_H}	specific heat capacity on hot side (kJ/kg K)
c_{p_C}	specific heat capacity on cold side (kJ/kg K)
D_h	hydraulic diameter (m)
ρ	density (kg/m^3)
μ	viscosity (Pa s)
λ	thermal conductivity (W/m K)
ΔP	pressure drop (Pa)
A_f	cross-sectional flow area (m^2)
L	actual flow channel length (m)
f	fanning factor
K	form loss coefficient
q''	heat flux (W/m^2)
h	heat transfer coefficient (W/m^2 K)
η	sum of squares
T	temperature (K)
T'	corrected temperature (K)
ΔT	temperature difference (K)
R_{Q_loss}	heat loss ratio
f	fanning friction factor
Re	Reynolds number
Nu	Nusselt number
Pr	Prandtl number
Subscript	
h	hot side
c	cold side
m	metal side
loss	loss
i	inlet
o	outlet
b	bulk mean
s	surface
p	pitch
_p	pitch
_A	volume A
_B	volume B
_C	volume C
_D	volume D
_0	cross-section 0
_1	cross-section 1
_2	cross-section 2
_3	cross-section 3
_4	cross-section 4

In this study, a He–CO_2 binary mixture was selected as a working fluid, because this binary mixture was one of candidates to increase overall thermal efficiency of HTGRs, which was mentioned by Jeong et al. [7]. Through a Mixture–Water test loop, we investigated the thermal–hydraulic performance of the PCHE. Using CFD code, FLUENT [8], the numerical investigations of thermal–hydraulic performance of the PCHE were performed under the mixture gas condition. Then, we compared the behaviors of Fanning factor and Nusselt number under mixture gas condition to those under single working fluids. The correlations of Fanning factor and Nusselt number were developed to predict pressure drop and heat transfer at the single working fluids as well as at the mixture gas.

2. Experimental approach

We constructed the Mixture–Water test loop in order to investigate thermal–hydraulic performance on a PCHE under the mixture gas condition. Pressures and temperatures were measured at the inlet and the outlet of the PCHE.

2.1. Mixture (He–CO_2) properties

For experiments, we selected the He–CO_2 binary mixture gas. Once calculating the mixture gas properties, several simple assumptions such as mole average, mass average, ideal gas law, and kinetic theory are sometimes used. However, we need to check if these assumptions provide accurate physical properties. The real properties of mixture gas with He of 0.8 mol and CO_2 of 0.2 mol at 1.5 MPa were provided according to temperatures from the REFPROP program of the NIST [9]. They were compared with the mixture gas properties calculated from the several simple assumptions. Depending on the assumptions, the mixture gas properties have large variation from the real mixture gas properties, as shown in Fig. 1. Since the use of accurate properties surely influences the reliability of data analysis and code calculations, we determined to use the real mixture gas properties provided from the REFPROP program.

However, the REFPROP program provides the properties of mixture gas with He and CO_2, only in the limited ranges of specific pressure, temperature, and concentrations. Fig. 2 shows the mixture properties at 1.3 MPa and 280 K in terms of He mole fraction. The real properties of mixture gas of are not linear according to the concentration. Even, the viscosity of the mixture gas with He of 0.8 mol and CO_2 of 0.2 mol does not lie between the viscosities of the pure He and CO_2. It is higher than those of pure He and CO_2.

2.2. Test range

The properties of mixture gas with He and CO_2 can be obtained from the REFPROP program, only in the limited ranges of specific pressure, temperature, and concentrations. We checked these ranges, which are shown in Table 1. Since the use of accurate property definitely relates with the reliability of data analysis and code calculations, we decided to perform the Mixture–Water tests in the specific ranges where the real properties of the mixture gas with He and CO_2 can be obtained from the REFPROP program of NIST.

2.3. Mixture–Water test loop

The Mixture–Water test loop constructed at KAIST is composed of a closed mixture gas loop and an open water loop (Fig. 3). After creating a vacuum state, the closed loop was charged with He and CO_2. The mixture gas was moved by a gas-bearing type circulator with no oil leakage. The hot mixture gas produced at a 150 kW heater was cooled in the PCHE as the heat on the hot side was released to the cold side. All residual heat was removed in the cooler. Purified water kept in a water tank was driven by a water pump. The water temperature increased in the PCHE as heat was transferred from the hot side to the cold side. The heated water was then vented out. The CO_2 gas concentration was measured by using a gas-analyzer as shown in Fig. 4.

The pressure was measured using a pressure transmitter with an accuracy of ±0.1%. The differential pressure gauge had an accuracy of ±0.2% over a full range of 100 kPa. The temperature was

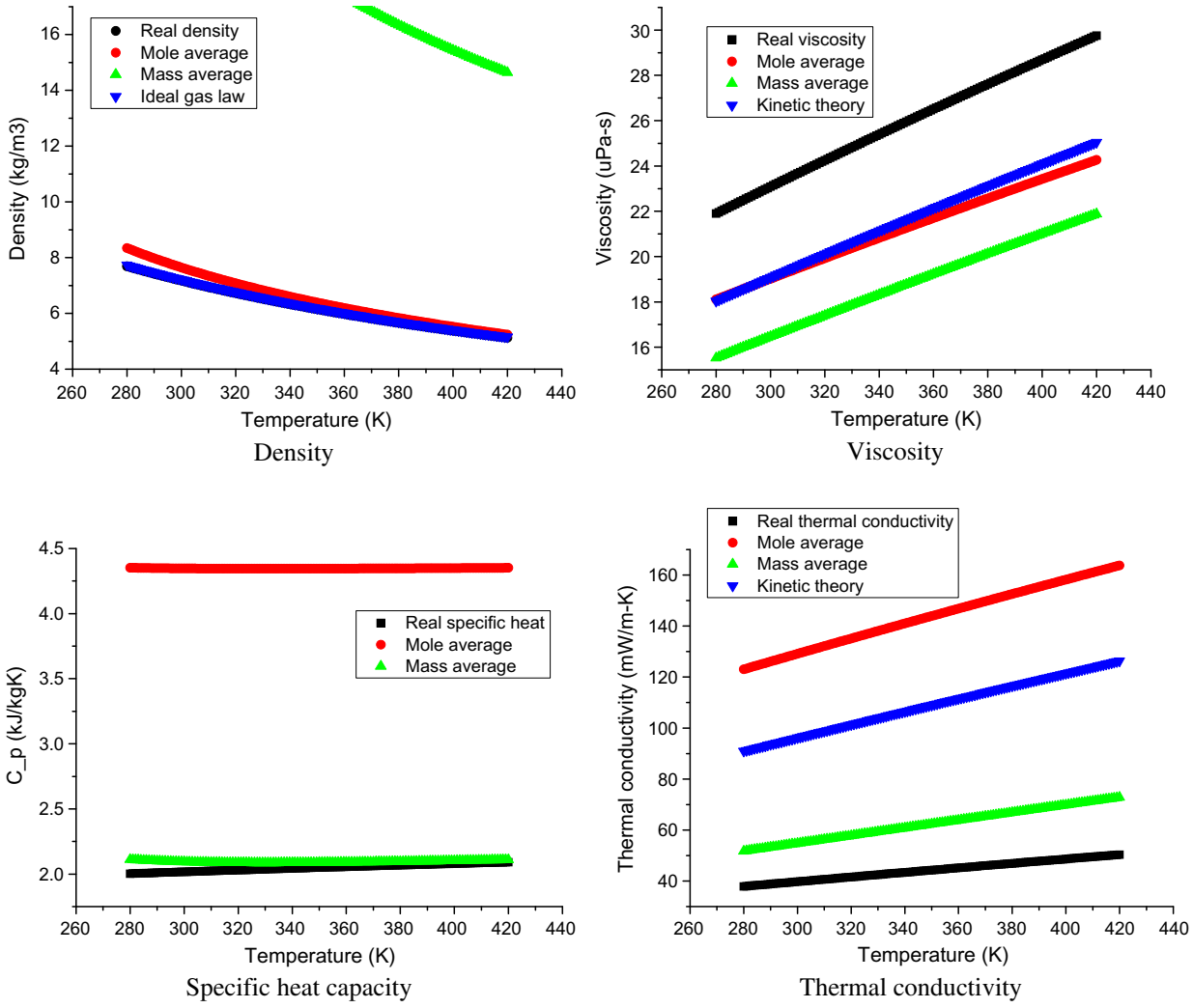

Fig. 1. Properties of mixture gas with He 0.8 mol and CO_2 0.2 mol at 1.5 MPa according to temperatures provided from the REFPROP and the simple assumptions.

measured using K-type thermocouples with an accuracy of ±1.6 °C. The inlet and outlet temperatures of the PCHE were measured by 1/16 in. thermocouples to increase the sensitivity. 1/8 in. thermocouples were used in the other sides. A vortex flow meter, whose accuracy was ±1% over a full scale of 13–130 m^3/h, was placed in the mixture gas side. A mass flow meter with ±0.5% accuracy was installed on the water side. The tested PCHE, made of Alloy 800HT by Heatric, is a countercurrent flow heat exchanger. It has 1280 micro-wavy channels with semi-circle shape on the hot and the cold sides, respectively. The geometry on both sides is identical. Its dry mass is 146 kg. The core dimension is 150 mm × 144 mm × 896 mm. Insulations were done to reduce heat loss. The geometry of a micro-wavy channel in the PCHE is shown in Fig. 5. The cross-section of the PCHE is in Fig. 6. Information on the PCHE structure is shown in Table 2 in detail. We performed the experiments for the vertical arrangement of PCHE.

In experiments, the mass flow rates of the mixture gas and the water were in the ranges of 0.0429–0.0914 kg/s and 0.108–0.546 kg/s. The hot/cold side inlet conditions for pressure and temperature were 1.17–1.72 MPa/0.104–0.306 MPa and 104.5–217.6 °C/23.6–25.2 °C, respectively. We measured the pressure and temperature at the inlet and outlet of the PCHE. The measured pressure drop includes five losses: inlet friction loss (from measurement location to inlet), inlet header loss, outlet header loss, outlet friction loss (from measurement to outlet), and pressure drop in the wavy channel. We focused on the pressure drop in the wavy channel only. It is calculated by difference between the measured total pressure drop and the estimated pressure drop due to four losses of inlet friction loss, inlet header loss, outlet header loss, and outlet friction loss. The estimated pressure drop due to inlet friction loss, inlet header loss, outlet header lose, and outlet friction loss were 9.59–22.49% for the mixture gas and 0.74–7.18% for the water side, compared to the total measured pressure drop. The sum of surface area in both inlet header and outlet header is approximately 4% of total surface area.

2.4. Heat loss analysis

In reality, the heat transfer in the hot side is not equal to that in the cold side due to the heat loss. Considering the heat balance, we need to understand the heat transfer behavior in the PCHE in advance. As shown in Fig. 7, the heat is transferred from the hot side to the metal solid. Then, it is transferred to either the cold side or the outside. Accordingly, we can set up some equations below:

$$Q_h = Q_m \tag{1}$$

where

$$Q_h = \dot{m}_h c_{p\_H}(T_{h,i} - T_{h,o})$$

$$Q_m = Q_c + Q_{loss} \tag{2}$$

where

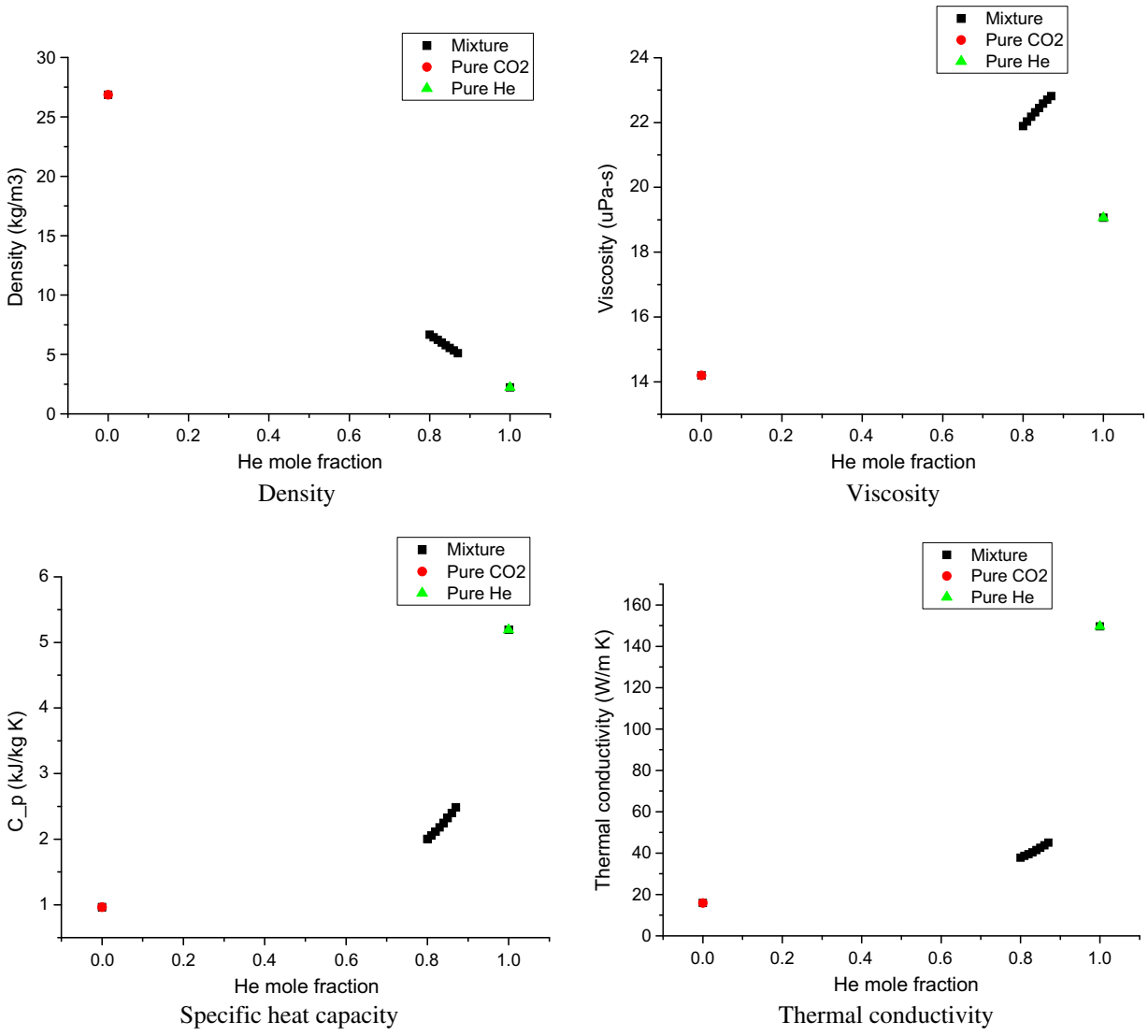

Fig. 2. Real mixture gas properties with He and CO_2 at 1.3 MPa and 280 K in terms of He mole fraction.

Table 1
Specific ranges where the mixture gas properties can be provided from REFPROP.

Helium mole fraction (x)	CO_2 mole fraction ($1-x$)	Pressure (MPa)	Temperature (K)	Mixture property
0.80	0.20	1–1.7	280–427	Obtainable
0.84	0.16	0.4–1.7	280–348	Obtainable
0.87	0.13	0.3–1.7	280–289	Obtainable
0.92	0.08	0.1–1.2	–	–
0.96	0.04	0.1–0.7	–	–
0.99	0.01	0.1–0.3	–	–

$$Q_c = \dot{m}_c c_{p\_C}(T_{c,o} - T_{c,i})$$

$$R_{Q\_loss} = \frac{Q_{loss}}{Q_h} \quad (3)$$

In our experiments, the range of the heat loss ratio was between 13.96% and 19.02%, although insulation was done. We think that most of heat loss came from the conduction heat losses at the end parts of hot locations through the hot inlet/cold outlet side tubes and the instrumentation tubes for pressure and temperature measurements. Considering the heat balance, the outlet temperature in the cold side is corrected using the following equation:

$$T'_{c,o} = T_{c,o} + \Delta T_{c,o} \quad (4)$$

where

$$Q_{loss} = \dot{m}_c c_{p\_C} \Delta T_{c,o}$$

3. Numerical approach

Since the channel in the PCHE is very small with the diameter of 1.51 mm, the measurements of internal pressure and temperature in the PCHE are not possible during experiments. Therefore, we used a numerical approach to compensate for the deficiencies in the experiments. We can obtain not only the inlet and outlet information but also the internal information from the results of numerical simulations. However, in advance, our numerical model should be validated against experimental data.

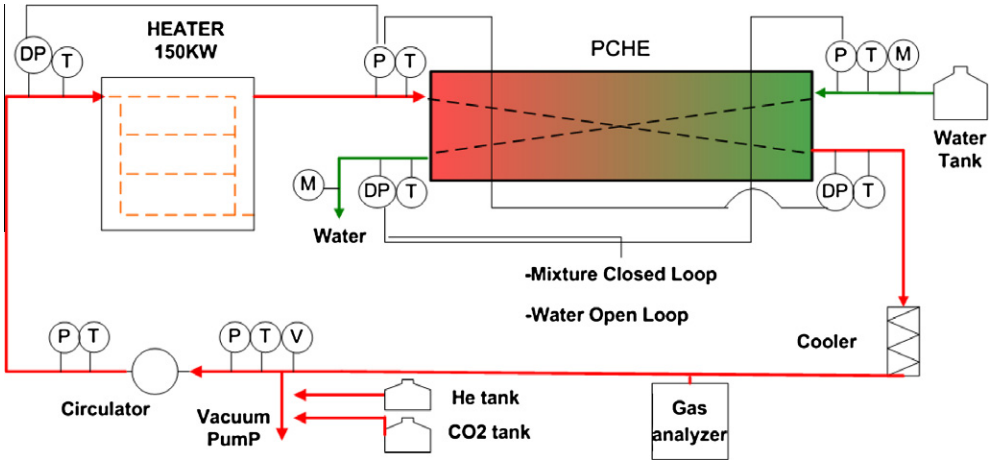

Fig. 3. Mixture–Water test loop.

Fig. 4. Gas analyzer.

3.1. Three-dimensional (3-D) numerical model

The construction of the entire structure of the PCHE requires many computer resources and much time for the simulations. In order to simplify the 3-D numerical model, since the arrangement of the channels was periodically repeated, we used periodic boundary conditions as shown in Fig. 8 under the assumption of the same mass flow rate, pressure, and temperature at each channel.

The cross-section of the 3-D model was reduced to a single-pair stack of 2.62 mm × 2.92 mm using a periodic boundary condition at top/down and left/right positions. Each single channel in the hot and the cold was constructed as the transparent full-channel length (742 mm) was maintained. GAMBIT was used to generate the structure and meshes. Checking several cases according to the mesh number, we determined the appropriate mesh number

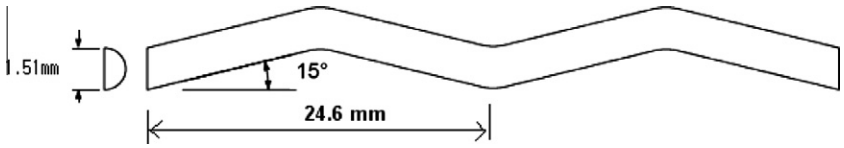

Fig. 5. Geometry of micro-wavy channel in the PCHE [5].

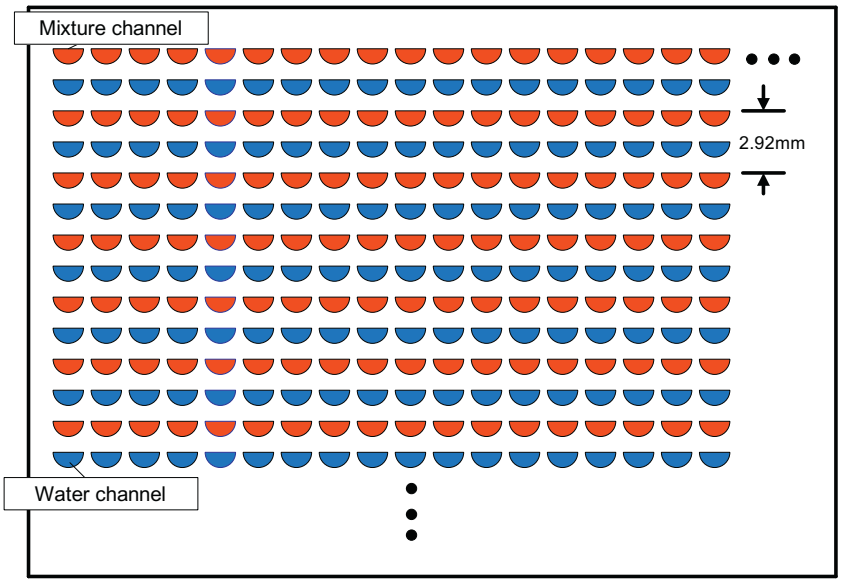

Fig. 6. PCHE cross-section.

Table 2
PCHE geometrical information.

Side	Number of channels	Diameter (mm)	Hydraulic diameter (mm)	Heat transfer area (m^2)	Cross-sectional flow area (m^2)	Wavy channel length (mm)	Angle (°)	Pitch (mm)
Mixture	40 × 32 = 1280	1.51	0.922	3.8	0.001155	765	15	24.6
Water	40 × 32 = 1280	1.51	0.922	3.8	0.001155	765	15	24.6

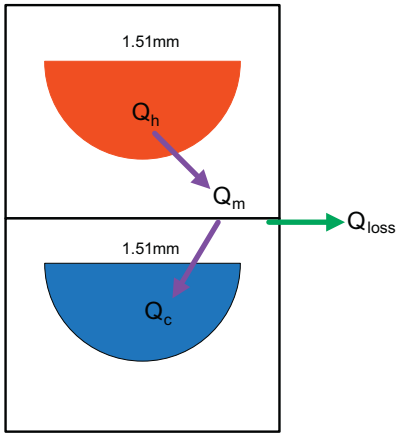

Fig. 7. The heat transfer behavior in the PCHE.

for our situation. The boundary layer option was used at the interface between the solid and the fluid. The first layer was 0.01 mm. Five rows were constructed with a growth factor of 1.2. The total depth was 0.0744 mm. The total number of generated meshes was approximately 1,330,000.

3.2. Numerical solution

The numerical solutions to the Mixture–Water tests with the vertical arrangement of the PCHE were obtained by using FLUENT. The governing equations of continuity, momentum, and energy were solved simultaneously using the first order upwind scheme. The semi-implicit method pressure-linked equation (SIMPLE) was used to couple the velocity and the pressure. The mass flow inlet and pressure outlet boundary conditions were selected for the mixture and the water sides, respectively. Thermo-physical properties (viscosity, density, specific heat, and thermal conductivity) of the binary mixture (He–CO_2) gas and water were obtained from the REFPROP and the NIST chemistry web-book [10]. The thermo-physical properties have considerable variation and significantly depend on the temperature. They were presented with a polynomial function of the temperature. The thermal conductivity of Alloy 800HT according to its temperature was obtained from the website [11].

4. Experimental data vs. numerical solutions

The differences between the experimental data and the numerical solutions were observed. The differences in the pressure and the temperature of the hot/cold sides between the experimental data and the numerical solutions were evaluated using the following equation:

$$\text{Error}(\%) = \frac{\text{CFD} - \text{Experiment}}{\text{Experiment}} \times 100 \quad (5)$$

For the Mixture–Water tests with the vertical arrangement of PCHE, the difference of the pressure drop and the temperature difference between experimental data and numerical solutions were in Figs. 9a and 9b.

Their RMS errors were calculated, as shown in Table 3. In Table 3, Hot and Cold, and DP and DT represent hot side and cold side, and pressure drop and temperature difference, respectively. On the water side, a little bit large RMS errors were obtained. The temperature difference on the cold side had a RMS error of 6.289%, which was less than ±1.6 °C of the thermocouple uncertainty. The pressure drop on the cold side had a RMS error of 12.68%. This phenomenon is similar to that in the previous He–Water tests by Kim and

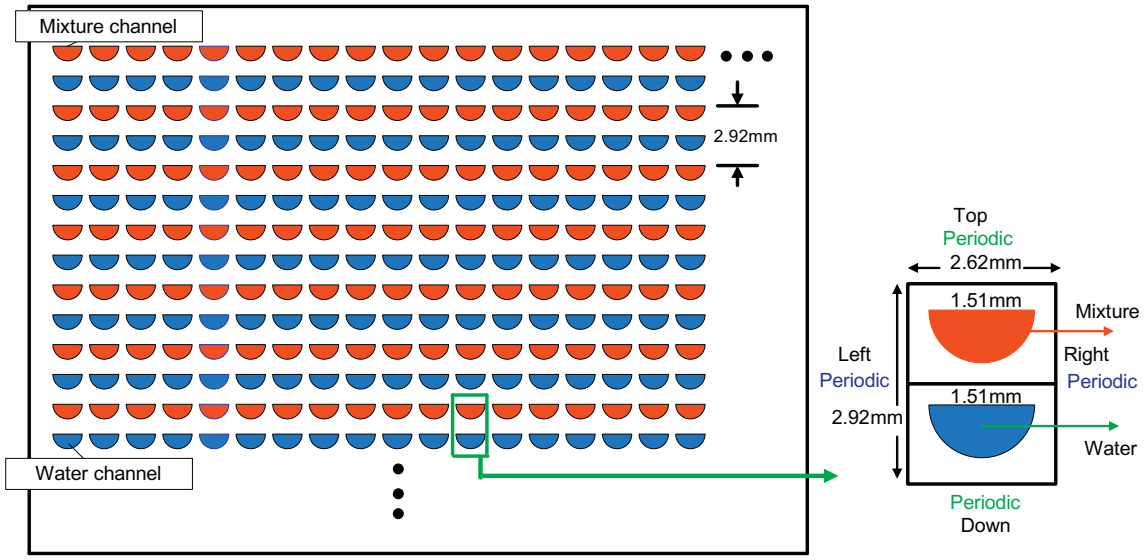

Fig. 8. A simplified numerical model in the PCHE using periodic boundary conditions for Mixture–Water tests.

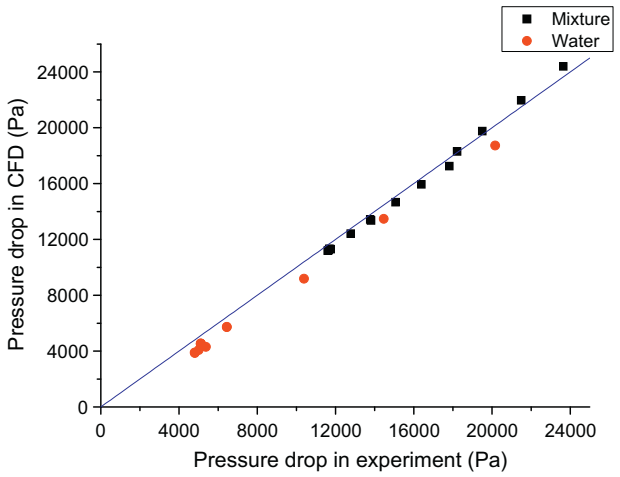

Fig. 9a. Pressure drop at the mixture and water sides of the PCHE (Experiments vs. CFD).

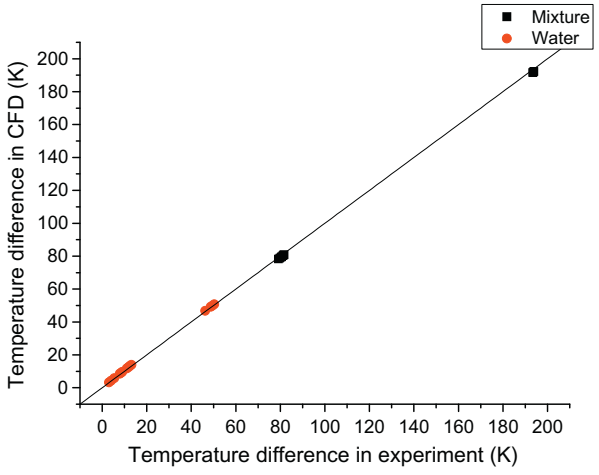

Fig. 9b. Temperature difference at the mixture and water sides of the PCHE (Experiment vs. CFD).

Table 3
RMS errors and maximum errors for the Mixture–Water tests.

	Hot DP (%)	Cold DP (%)	Hot DT (%)	Cold DT (%)
RMS error	2.884	13.68	1.039	6.289
Max error	3.864	20.07	1.206	8.592

NO [5] where the water side showed the larger variations than the helium side. The non-uniform flow in water side was the suggested reason. On the mixture side, pressures and temperatures provided from numerical solutions are in good agreement with experimental data. After this validation, we can use local information which is provided from numerical solutions.

5. Methodology for the correlation development

Two methods are available to develop correlations. One is using global parameters at the inlet and the outlet of PCHE. The other is using local parameters at the micro-wavy channel of PCHE. However, it was found that the local pitch-averaged correlation is more accurate than the global correlations, analyzing the heat exchanger system (Kim et al. [3]). This method is used in the He–He tests and the He–Water tests [3,5]. In spite of the identical Reynolds number and Prandtl number, the different Fanning factor and Nusselt number can be obtained according to the locations such as the curved and the straight. However, adopting the local-pitch averaged method, the location effect can be evenly distributed. Therefore, we can propose the correlations of Fanning factor and Nusselt number regardless of location effect. In addition, the property uncertainty can be lower, because temperature difference in a pitch gets lower than that in the total wavy channel with full length. The details in local pitch-averaged method [3,5] are shown below.

5.1. How to get local pitch-averaged values

This section explains how to get local pitch-averaged values. A pitch in a micro-wavy channel is shown in Fig. 10. A, B, C, D indicate volumes while 0, 1, 2, 3, 4 do cross-sections.

The bulk mean temperature in the cross-section 0, 1, 2, 3, 4 are mass weighted. The bulk mean temperature of volume A between 0 and 1 is defined by Eq. (6). Then, the local pitch-averaged bulk mean temperature is calculated by Eq. (7):

$$T_{b\_A} = \frac{T_{b\_0} + T_{b\_1}}{2} \tag{6}$$

$$T_{b\_p} = \frac{T_{b\_A} + T_{b\_B} + T_{b\_C} + T_{b\_D}}{4} \tag{7}$$

Fluid properties such as density, viscosity, and thermal conductivity were already presented with a polynomial function of temperature. As substituting local pitch-average bulk mean temperature, fluid properties are obtained.

Heat fluxes and surface temperatures are area-weighted. The heat flux and surface temperate in a pitch are calculated by the following equations:

$$q''_{s\_p} = \frac{q''_{s\_A} + q''_{s\_B} + q''_{s\_C} + q''_{s\_D}}{4} \tag{8}$$

$$T_{s\_p} = \frac{T_{s\_A} + T_{s\_B} + T_{s\_C} + T_{s\_D}}{4} \tag{9}$$

5.2. How to develop the local pitch-averaged correlations

The local pitch-averaged Fanning factor and Nusselt number were calculated by the following equations:

$$f_p = \frac{\Delta P_p \rho_p D_h A_f^2}{2 L_p \dot{m}^2} \tag{10}$$

$$Nu_p = \frac{h_{s\_p} D_h}{\lambda_p} = \frac{q''_{s\_p} D_h}{\lambda_p (T_{b\_p} - T_{s\_p})} \tag{11}$$

The local-pitch averaged Reynolds number and Prandtl number are defined by Eqs. (12) and (13), respectively, using the local pitch-averaged fluid properties:

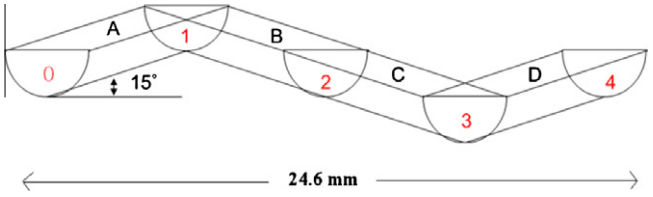

Fig. 10. Pitch configuration in a micro-wavy channel of the PCHE [5].

$$\mathrm{Re_p} = \frac{\rho v D_h}{\mu_p} = \frac{\dot{m} D_h}{A_f \mu_p} \tag{12}$$

where $\dot{m} = \rho v A_f$

$$\mathrm{Pr_p} = \frac{c_p \mu_p}{\lambda_p} \tag{13}$$

The pressure drop in the micro-channel of the PCHE consists of form loss and friction loss. The Fanning factor of the PCHE contains the form loss coefficient and the Fanning friction factor.

$$\Delta P_p = \Delta P_{form} + \Delta P_{friction} \tag{14}$$

$$\Delta P_p = 4 f_p \frac{L_p}{D_h} \frac{1}{2} \rho v^2 = 4 f_p \frac{L_p}{D_h} \frac{1}{2\rho} \left(\frac{\dot{m}}{A_f}\right)^2 \tag{15}$$

where $\dot{m} = \rho v A_f$

$$\Delta P_{form} = K \frac{1}{2} \rho v^2 \tag{16}$$

$$\Delta P_{friction} = 4 f \frac{L_p}{D_h} \cdot \frac{1}{2} \rho v^2 \tag{17}$$

where $f = 15.78/\mathrm{Re_p}$

A function of the Reynolds number in Eq. (18) is obtained for the Fanning factor multiplied Reynolds number through implementing Eqs. (15)–(17) into Eq. (14). In this paper, from now on, Re is considered as $\mathrm{Re_p}$. The Fanning factor correlation in the PCHE can be developed by observing $f_p \cdot \mathrm{Re}$ vs. Re behavior.

$$f_p \cdot \mathrm{Re} = 15.78 + \alpha \mathrm{Re}^{\beta} \tag{18}$$

We think it is reasonable that the fluid behavior is getting like a fully developed straight duct with a semi-circle cross-section as the Reynolds number is approaching 0. The Fanning factor multiplied Reynolds number and the Nusselt number reach approximately 15.78 and 4.089, respectively, shown in Table 4 [12]. The H1 thermal boundary condition is the axially constant wall flux with a circumferentially constant wall temperature.Therefore, the correlation form of Nusselt number is expressed in terms of the Reynolds number and the Prandtl number as shown in Eq. (19). Nu, Re, and Pr are considered as $\mathrm{Nu_p}$, $\mathrm{Re_p}$, and $\mathrm{Pr_p}$.

$$\mathrm{Nu} = 4.089 + k \mathrm{Re}^a \mathrm{Pr}^b \tag{19}$$

The Nusselt number correlation can be developed by finding the optimal constants of k, a, and b in the following equation:

$$\Delta \mathrm{Nu} = \mathrm{Nu} - 4.089 = k \mathrm{Re}^a \mathrm{Pr}^b \tag{20}$$

The three unknown values are calculated through multiple linear regressions [13]. A logarithmic equation described in Eq. (21) is obtained if the logarithm of the both sides of Eq. (20) is taken:

$$\Delta \ln(\Delta \mathrm{Nu}) = \ln k + a \ln \mathrm{Re} + b \ln \mathrm{Pr} \tag{21}$$

where $\ln k = k'$

The sum of squares is defined by using the following equation:

$$\eta = \sum_{i=1}^{N} [\ln(\Delta \mathrm{Nu}) - \ln(\Delta \mathrm{Nu_i})]^2 = \sum_{i=1}^{N} \left[\ln\left(\frac{\Delta \mathrm{Nu}}{\Delta \mathrm{Nu_i}}\right)\right]^2 \tag{22}$$

Table 4
Fanning factor and Nusselt number in a fully developed straight duct with a semi-circle cross section [12].

Cross-section	$f \cdot \mathrm{Re}$	Nu (H1 boundary condition)
Circle	16	4.364
Semi-circle	15.78	4.089

The optimal constants of k', a, and b can be calculated when satisfying Eq. (23), which means the sum of squares is minimized.

$$\frac{\partial \eta}{\partial k'} = \frac{\partial \eta}{\partial a} = \frac{\partial \eta}{\partial b} = 0 \tag{23}$$

The equations are simplified to the matrix form below in Eq. (24). Nusselt number correlation was developed by obtaining the optimal constants of k', a, and b.

$$\begin{pmatrix} \sum 1 & \sum \ln \mathrm{Re_i} & \sum \ln \mathrm{Pr_i} \\ \sum \ln \mathrm{Re_i} & \sum (\ln \mathrm{Re_i})^2 & \sum (\ln \mathrm{Re_i} \cdot \ln \mathrm{Pr_i}) \\ \sum \ln \mathrm{Pr_i} & \sum (\ln \mathrm{Re_i} \cdot \ln Pr_i) & \sum (\ln \mathrm{Pr_i})^2 \end{pmatrix} \begin{pmatrix} k' \\ a \\ b \end{pmatrix} = \begin{pmatrix} \sum \ln \Delta \mathrm{Nu_i} \\ \sum (\ln \Delta \mathrm{Nu_i} \cdot \ln \mathrm{Re_i}) \\ \sum (\ln \Delta \mathrm{Nu_i} \cdot \ln \mathrm{Pr_i}) \end{pmatrix} \tag{24}$$

6. Physical correlations

For the mixture gas, we obtained dimensionless parameters such as Reynolds number, Fanning factor and Nusselt number through the local pitch-averaged approach. These values from the mixture gas were compared with those previously provided from the He–He tests and the He–water tests [3,5].

6.1. Fanning factor correlation

Under the same PCHE geometry, we collected the thermal–hydraulic performance data according to the working fluids such as the helium, the water, and the mixture gas. In order to compare the Fanning factor of mixture gas with that previously suggested in He–He tests and He–Water tests [3,5], we draw Fig. 11. The behavior of the Fanning factor in the mixture gas is similar to that in the single working fluids such as the helium and the water.

The correlation developed previously by using the data of the helium and the water [3,5] only is Eq. (25).

$$f_p \cdot \mathrm{Re} = 15.78 + 0.0487 \mathrm{Re}^{0.84}, \quad 0 < \mathrm{Re} < 2500 \tag{25}$$

However, to suggest more accurate correlation covering the helium, the water, and the mixture gas, we propose the following

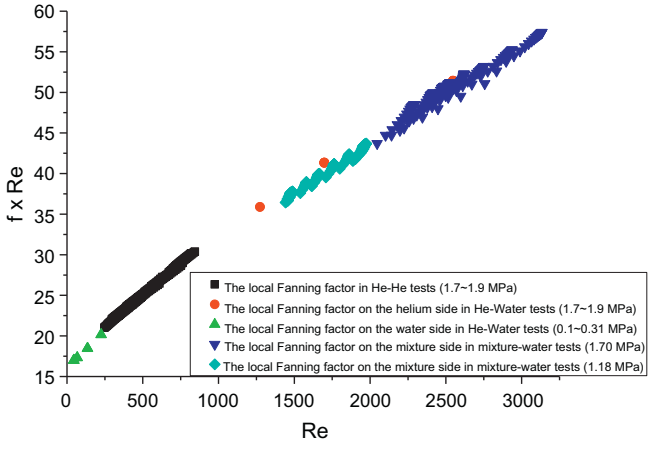

Fig. 11. Fanning factor vs. Re from He–He tests [3], He–Water tests [5], and Mixture–Water tests.

Fanning factor correlation for the tested PCHE with 1.37% of the calculated RMS error:

$$f_p \cdot \mathrm{Re} = 15.78 + 0.0557\mathrm{Re}^{0.82},$$

$$0 < \mathrm{Re} < 3000 \tag{26}$$

6.2. Nusselt number correlation

We got the following Nusselt number correlation, which was developed previously considering the data of the He–He tests [3] and the He–Water tests [5]:

$$\mathrm{Nu} = 4.089 + 0.00365 \cdot \mathrm{Re}^{1.00} \cdot \mathrm{Pr}^{0.58}$$

$$0 < \mathrm{Re} < 2500, 0.66 < \mathrm{Pr} < 13.41 \tag{27}$$

Adopting this correlation for mixture gas, we can predict the Nusselt number in the mixture gas within the 6.11%. However, in order to develop a more accurate Nusselt number correlation, we performed multiple regressions using the data of the He–He tests [3], the He–Water tests [5], and the Mixture–Water tests. Finally, we suggested the Nusselt number correlation for the tested PCHE as shown in Eq. (28). The calculated RMS error of this correlation was 3.98%.

$$\mathrm{Nu} = 4.089 + 0.00497 \cdot \mathrm{Re}^{0.95} \cdot \mathrm{Pr}^{0.55},$$

$$0 < \mathrm{Re} < 3000, 0.66 < \mathrm{Pr} < 13.41 \tag{28}$$

7. Conclusions

We investigated thermal–hydraulic performance of the PCHE using the Mixture–Water test loop. The numerical solutions were provided by using CFD code FLUENT. The Fanning factor and the Nusselt number were obtained through the local approach. We collected the data of Fanning factor and the Nusselt number using the He–He tests, the He–Water tests, and the Mixture–Water tests. Then, covering the data of the helium, the water, and the mixture gas, we proposed the correlations of Fanning factor and Nusselt number for the tested PCHE. Finally, we can conclude that regardless of pressure, temperature, gas types, and mixing concentrations, we can obtain the single Fanning factor correlation and the single Nusselt number correlation for the same PCHE channel geometry using the suggested procedure.

Acknowledgements

The authors gratefully acknowledge that this research was supported by Grant No. EEWS-2012-N01120021 from the EEWS research project of the office of KAIST EEWS (Energy, Environment, Water, and Sustainability) initiative.

References

[1] H.C. NO et al., Conceptual design and experimental validation of core technologies for WHEN (Water-Hydrogen-Electricity Nuclear reactor) system, Ministry of Education, Science and Technology (MEST) report 2010-0020421, 2011
[2] Heatric web-page: <http://www.heatric.com/compactness_heat_exchanger.html>.
[3] I.H. Kim, H.C. NO, J.I. Lee, B.G. Jeon, Thermal hydraulic performance analysis of the printed circuit heat exchanger using a helium facility and CFD simulations, Nucl. Eng. Des. 239 (2009) 2399–2408.
[4] I.H. Kim, H.C. No, Physical model development and optimal design of PCHE for intermediate heat exchangers in HTGRs, Nucl. Eng. Des. 243 (2012) 243–250.
[5] I.H. Kim, H.C. NO, Thermal hydraulic performance analysis of a printed circuit heat exchanger using a helium–water test loop and numerical simulations, Appl. Therm. Eng. 31 (2011) 4064–4073.
[6] M.S. El-Genk, J-M. Tournier, Noble gas binary mixtures for gas-cooled reactor power plants, Nucl. Eng. Des. 238 (2008) 1353–1372.
[7] W.S. Jeong, J.I. Lee, Y.H. Jeong, H.C. No, Potential improvements of supercritical CO_2 Brayton cycle by mixing other gases, ICAPP2010, June 13–17, San Diego, CA, USA, 2010, Paper 10237.
[8] FLUENT 6.3.26.
[9] E.W. Lemmon, M.L. Huber, M.O. McLinden, NIST Standard Reference Database 23: Reference Fluid Thermodynamic and Transport Properties-REFPROP, Version 8.0, National Institute of Standards and Technology, Standard Reference Data Program, Gaithersburg, 2007.
[10] NIST web-page: <http://webbook.nist.gov/chemistry/fluid>.
[11] Special Metal Web-page: <http://www.specialmetals.com>.
[12] J.E. Hesselgreaves, Compact Heat Exchanger, Pergamon, 2001. pp. 156–160.
[13] W. Huge, W. Coleman, J.R. Glenn Steele, Experimentation and Uncertainty Analysis for Engineers, A Wiley-Interscience Publication John Wiley & Sons, Inc., New York, 1999. pp. 229–231.